Identifying Over-Production of Elements in GCE for Milky Way Model

Ben F. Rasmussen[1]★
[1]*Department of Physics and Astronomy, University of Victoria, 3800 Finnerty Rd, Victoria, BC V8P 5C2, CA*

Accepted 2024 April 24th. Received 2024 April 24th;

ABSTRACT
By modelling the chemical evolution of a galaxy with conditions leading to optimized yields consistent with that of the Milky Way, anomalous production of elements were identified with unusually large [X/Fe] abundances at [Fe/H] ≈ 0. Using the OMEGA+ code for multi-zone galactic chemical evolution modelling with NuGrid stellar yields as input, indicated an over-production of five elements with respect to solar abundances. These elements were found to be Cr, Zr, Co, Ni, and Cl. To investigate the source of the increase of these species, the SYGMA code demonstrated that the nature of surplus of each was different; Chromium ($M = 20M_\odot, Z = 0.01$) and Zirconium ($M = 15M_\odot, Z = 0.006$) were found to be sourced from single NuGrid models while Chlorine ($M = 15M_\odot, Z = 0.01, 0.02$) came from two models. Cobalt and Nickel seem to be systemically over-produced across various stellar input models. The Chromium abundance spike is attributed to the merging of Si-burning and C-burning shells rich in Chromium outside of the remnant mass coordinate prior to core collapse supernova. Zirconium appears to be added in excess to the model due to a neutron-rich Ne-burning convective shell outside of the models respective remnant mass coordinate. The discrepancy between the model and observations suggests that these mechanisms are either non-physical or contribute far too much to the overall model.

Key words: nuclear reactions – nucleosynthesis – abundances – Galaxy: stellar content – galaxies: star formation

INTRODUCTION

Modelling the chemical evolution of galaxies like the Milky Way allows us to combine the theoretical frameworks of nuclear astrophysics with the most recent observational data (Matteucci 2014; Côté et al. 2020; Côté et al. 2017). Galactic chemical evolution (GCE) models are a synthesis of the initial conditions of the interstellar medium and the stars within, the rate of creation of newly formed stars, the flow of gas in and out of the population, and the specifics of the elemental yields produced by members of the stellar population (Matteucci 2014). The ingredients in a GCE simulation involve a multi-disciplinary approach involving nuclear astrophysics, the evolution of stars and groupings of stars, and cosmology which can be compared with astronomical observations to improve our understanding of the formation of, not only galaxies, but the elements and the way they are utilized by nature and put back into inter-stellar and inter-galactic space (Côté et al. 2017). These models are a difficult task to perform properly, due to the extreme scales involved combined with our limited understanding of certain processes and lack of computing power (Côté et al. 2016, 2020). As mentioned, one of the fundamental building blocks of GCE is the stellar yields that are recycled back into the model (Côté et al. 2020). Since there is uncertainty associated with these yields and their contributions to the model as a whole, it is important to identify shortcomings in the stellar yields utilized by the model (Côté et al. 2016, 2017, 2020)

Since we have considerable observational constraints on the parameters associated with GCE models for the Milky Way, theoretical models of its evolution are fundamental to our understanding of how it formed (Alibés, A. et al. 2001; Gibson et al. 2003). Using these constraints, we may subsequently impose constraints, or at least identify outcomes that do not match observation, for the underlying stellar models providing the yields (Côté et al. 2020; Ritter et al. 2018b).

As done previously (Côté et al. 2020), there are elements produced by GCE modelling that are considerably anomalous with respect to observations made in our galaxy. It is of interest here to then reproduce these inconsistencies and expand the scope to any element that exhibits over-production with the given stellar yields with respect to observations. The work presented here is a partial recreation of Côté et al. (2020) with a focus on the identification of stellar yields that overshoot the constraints of observation. A cursory description of the source of the overproduction will be done for the primary element from Côté et al. (2020) as well as other identified elements but is limited in its scope of explanation.

This paper will describe the methods used to create an accurate GCE model as well as identify the elements that are produced in excess for such a model. In doing so, the exact models that cause the unexpected elemental overproduction are found and an attempt to explain why the particular model sources act as they do will be undertaken.

METHODS

Modelling of the galactic chemical evolution of the Milky Way was performed using the OMEGA+ code which acts as a multi-zone GCE code that includes both a galactic (star-forming gas) and circumgalactic (hot gas reservoir) component in its modelling (Côté et al. 2017). This code is part of the JINAPyCEE environment (Côté et al. 2017).

★ Contact e-mail: benfrasmussen@uvic.ca

To generate an accurate model, the input parameters were optimized to fall within the uncertainties associated with Milky Way observations for the following parameters at current time: Star formation rate [$SFR \approx 2M_{\odot}/yr$], interstellar medium gas mass [$M_g \approx 7 \cdot 10^9 M_{\odot}$], galactic inflow rate [$\approx 1M_{\odot}/yr$], and most importantly, the solar iron abundance at the time of the sun's formation [$[Fe/H] \approx 0$]. With an accurate model, the output yields of elements were analyzed to identify species that were markedly over-produced in the model when compared to observation (Bensby et al. 2014; Battistini & Bensby 2015; Battistini, Chiara & Bensby, Thomas 2016). The observational abundances were found using STELLAB (Ritter & Côté 2016a). As mentioned previously, the stellar yield inputs from Ritter et al. (2018b) form the basis of the GCE model, and the specific input stellar models resulting in over-productions were probed using the SYGMA code (Ritter et al. 2018a).

RESULTS

When comparing the model abundances at $[Fe/H] \approx 0$ or roughly the time of solar formation, we find that five elements are present in the model in quantities inconsistent with the necessary background conditions to produce solar abundances. These elements are Cr, Zr, Co, Ni, and Cl and the NuGrid models (Ritter et al. 2018b) responsible for sourcing the excess can be seen in Table 1; all five elements are primarily produced in massive stars. Of note is that Chromium and Zirconium production is dominated by single mass and metallicity stellar models suggesting a need to investigate these particular cases. Chromium is fed into the GCE model by a single ($M = 20M_{\odot}, Z = 0.01$) stellar model (Côté et al. 2020) while Zirconium is sourced by a different ($M = 15M_{\odot}, Z = 0.006$) star. Cobalt and Nickel are both produced in large quantities in massive stars ($M_* > 5M_{\odot}$ across the available metallicities from NuGrid (Ritter et al. 2018b). Chlorine is split between two stellar models of about equal contribution ($M = 15M_{\odot}, Z = 0.01, 0.02$) that do not show quite as significant order of magnitude increase for these models compared to the rest.

Fig 1 shows the predicted evolution of each of these elemental abundances, $[X/Fe]$, as a function of $[Fe/H]$. Near $[Fe/H] \approx 0$, each of these identified elements have different behaviour but are all inconsistent with Milky Way disk observations (Bensby et al. 2014; Battistini & Bensby 2015; Battistini, Chiara & Bensby, Thomas 2016) shown in cyan. Chromium exhibits approximately a half order of magnitude increase at around $[Fe/H] = 0$, due to the core collapse supernova of the single stellar model found above ($M = 20M_{\odot}, Z = 0.01$) which is consistent with the results from Côté et al. (2020) but only reaches about half of the total increase, likely due to changes in the simulation parameters. In addition, we see a considerable spike in Zirconium production in pre-solar times that fades closer to $[Fe/H] = 0$. This is also due to a single model ($M = 15M_{\odot}, Z = 0.006$) core collapse supernova. Of note is that the observational constraints on the evolutionary tracks of the Cr and Zr are different, in that Chromium has less uncertainty and Zirconium follows a downward trend with considerable spread as seen in Fig. 1. Cobalt and Nickel both do not have a spike due to an event from any of the NuGrid models (Ritter et al. 2018b) and as such, their over-production is likely due to systemic discrepancies in the models. Finally, Chlorine also exhibits a noticeable spike around $[Fe/H] = 0$ likely due to the two models ($M = 15M_{\odot}, Z = 0.01, 0.02$) found but no observational disk data was obtained for this element in Ritter & Côté (2016a). Since we can trace the origin of the anomalous production of both Cr and Zr to single, tractable models while the other three are either more complex or missing components, we then proceed by analyzing the source of Cr and Zr. We now look to understand the mechanisms present in the stellar interiors of the models responsible. To do so, Kippenhahn diagrams for both the Cr model and the Zr model can be seen in Fig. 2 and Fig. 3. Looking to Fig. 2 we see the presence of a considerable convection zone in the times before core collapse. This convection zone is in fact a shell merger of Carbon and Silicon burning zones that can be seen in the bottom of the same figure, between the mass coordinates of $\approx 1.3M_{\odot}$ and $\approx 5M_{\odot}$. Stars of this mass and metallicity will collapse into black holes, ejecting the majority of their mass back out into the interstellar medium but leave behind a remnant mass (Fryer et al. 2012). Following the procedure outlined in (Fryer et al. 2012), we find that the size of the remnant black hole will be $\approx 2.77M_{\odot}$ and anything outside of this will be ejected. The maroon lines in Fig. 2 correspond to this value, which falls well within the convection zone comparable to the results of (Côté et al. 2020). This convection zone is rich in Chromium and so we see that the merger of the two burning shells cause this excess Chromium to be ejected back into the interstellar medium, causing the spike in Fig. 1. In a similar way, we look at the progenitor of the overproduction of Zirconium in Fig. 3. There exists a convective zone of a likely Neon burning shell that sits above the remnant mass coordinate of $\approx 1.61M_{\odot}$ found with results from Fryer et al. (2012). This shell is rich in Neon with Magnesium present allowing for the

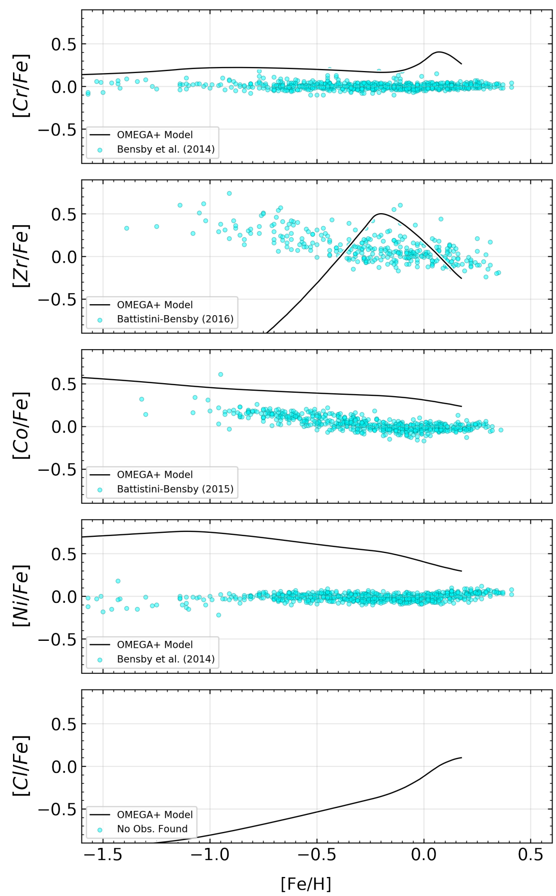

Figure 1. Modelled evolution of $[X/Fe]$ as a function of $[Fe/H]$ for the five identified elements (Cr, Zr, Co, Ni, Cl) that display overproduction in the OMEGA+ GCE model (Côté et al. 2017) with NuGrid yields as input (Ritter et al. 2018b). Observational data from (Bensby et al. 2014), (Battistini & Bensby 2015), and (Battistini, Chiara & Bensby, Thomas 2016).

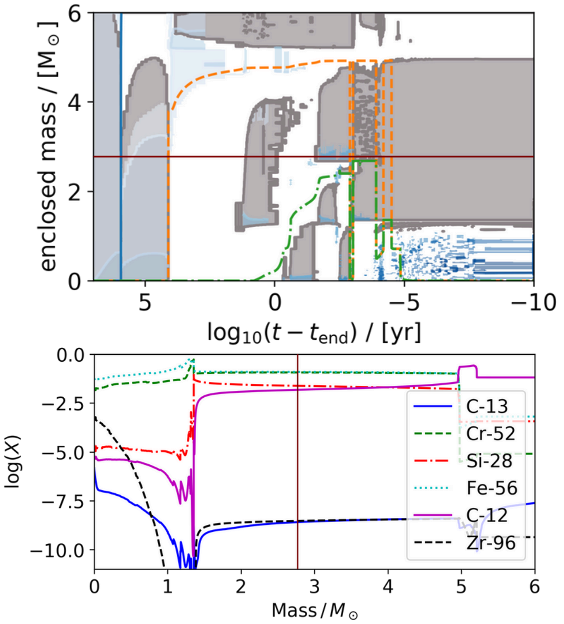

Figure 2. *Top*: Kippenhahn (convective structure evolution) diagram (Côté et al. 2020) for the inner region ($< 6M_\odot$) of the $20M_\odot, Z = 0.01$ NuGrid model with the logarithmic time before collapse along the x-axis. This model corresponds to the source of the Cr over-production. The collapsed remnant mass cut of $2.77M_\odot$ (Fryer et al. 2012) is the horizontal line in maroon. *Bottom:* Abundance profile plot of the same NuGrid data for the model immediately prior to core-collapse. In Si/C-burning convection zone $[Cr/Fe] \approx 0$. The mass coordinate of the mass cut is the vertical maroon line.

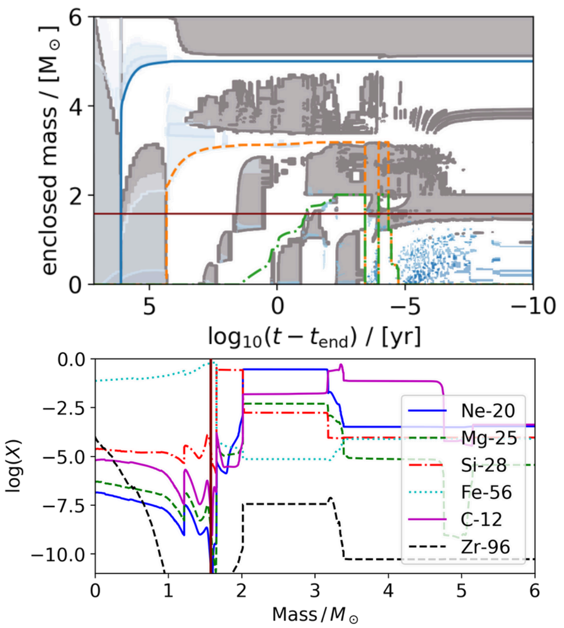

Figure 3. *Top*: Kippenhahn (convective structure evolution) diagram (Côté et al. 2020) for the inner region ($< 6M_\odot$) of the $15M_\odot, Z = 0.006$ NuGrid model with the logarithmic time before collapse along the x-axis. This model corresponds to the source of the Zr over-production. The collapsed remnant mass cut of $1.61M_\odot$ (Fryer et al. 2012) is the horizontal line in maroon. *Bottom:* Abundance profile plot of the same NuGrid data for the model immediately prior to core-collapse. The mass coordinate of the mass cut is the vertical maroon line.

Element:	Primary Source:	Model(s):
Cr	Massive Stars	$M = 20M_\odot,\ Z = 0.01$
Zr	Massive Stars	$M = 15M_\odot,\ Z = 0.006$
Co	Massive Stars	$M = 10, 15M_\odot,\ Z = All$
Ni	Massive Stars	$M = 10, 15M_\odot,\ Z = All$
Cl	Massive Stars	$M = 15M_\odot,\ Z = 0.01, 0.02$

Table 1. Nucelosynthetic source (Ritter et al. 2018a) and NuGrid models (Ritter et al. 2018b) that contribute to the overproduction of a given element.

$^{22}Ne(\alpha, n)^25Mg$ reaction to occur as a source of neutrons in the shell (van Raai, M. A. et al. 2012). The weak s-process can then occur, producing elements up to a magic number of 50 and so we see an increase in the production of Zirconium via neutron capture in this region in the bottom of Fig. 3 (van Raai, M. A. et al. 2012). This entire shell is then ejected back into the ISM above the black hole mass cut.

DISCUSSION

Using the OMEGA+ code (Ritter & Côté 2016b), five overproduced elements were identified with two being from single NuGrid stellar models, two from systemic excess across multiple NuGrid models and one from two models but without sufficient observational constraints. The results from Côté et al. (2020) were recreated, demonstrating that the overproduction in Cr is due to a C/Si-shell merger hours before supernova (Côté et al. 2020). In addition, Zirconium production was found due to a neutron-rich Ne-burning shell outside of the remnant black hole mass cut. The yields from these models ejected back out into the ISM are inconsistent with observations of the Milky Way. For Cr (and the others apart from Zr), these anomalous results are not found in other GCE models (Alibés, A. et al. 2001). Similarly, it is not found for Zr either (Grisoni et al. 2020). As the majority of elements in our GCE model match observations well, it is then likely that either the yields from NuGrid for Cr and Zr are incorrect for the single stellar model or the mechanisms behind the source of Cr and Zr overproduction in the models are nonphysical events (Côté et al. 2020).

CONCLUSIONS

We have identified five elements where their respective production is anomalous with respect to observations. Two of these elements can be traced to single NuGrid models behaving in interesting ways (Ritter et al. 2018b; Côté et al. 2020). The model that produces Chromium in excess is a $20M_\odot$, $Z = 0.01$ stellar model while Zirconium is produced within a $15M_\odot$, $Z = 0.006$ model. As the identification of the five overproduced elements (Cr, Zr, Co, Ni, Cl) has been completed, a detailed description of the mechanisms behind it is then necessary but are outside the scope of this paper [see Côté et al. (2020)]. In addition, a number of elements were considerably *underproduced* in the model, which are far more difficult to diagnose but would motivate further look into any shortcomings with the NuGrid yields. Answering these questions would give us a better understanding of the relationship between the way galaxies evolve chemically and the constituent elemental stellar yields constrained by astronomical observations.

ACKNOWLEDGEMENTS

Thank you to Dr. Falk Herwig for providing both the idea behind this project and the resources necessary to produce the presented results. In addition, thank you for a truly engaging and interesting course; I have learned a ton.

DATA AVAILABILITY

The data and simulation output used here is available upon request.

REFERENCES

Alibés, A. Labay, J. Canal, R. 2001, A&A, 370, 1103

Battistini C., Bensby T., 2015, Astronomy & Astrophysics, 577, A9

Battistini, Chiara Bensby, Thomas 2016, A&A, 586, A49

Bensby T., Feltzing S., Oey M. S., 2014, Astronomy & Astrophysics, 562, A71

Côté B., Ritter C., O'Shea B. W., Herwig F., Pignatari M., Jones S., Fryer C. L., 2016, ApJ, 824, 82

Côté B., O'Shea B. W., Ritter C., Herwig F., Venn K. A., 2017, ApJ, 835, 128

Côté B., Jones S., Herwig F., Pignatari M., 2020, ApJ, 892, 57

Côté B., Ritter C., Herwig F., O'Shea B. W., Pignatari M., Silvia D., Jones S., Fryer C. L., 2017, in Proceedings of the 14th International Symposium on Nuclei in the Cosmos (NIC2016). Journal of the Physical Society of Japan, doi:10.7566/jpscp.14.020203, `http://dx.doi.org/10.7566/JPSCP.14.020203`

Fryer C. L., Belczynski K., Wiktorowicz G., Dominik M., Kalogera V., Holz D. E., 2012, The Astrophysical Journal, 749, 91

Gibson B. K., Fenner Y., Renda A., Kawata D., Lee H.-c., 2003, Publications of the Astronomical Society of Australia, 20, 401–415

Grisoni V., Cescutti G., Matteucci F., Forsberg R., Jönsson H., Ryde N., 2020, Monthly Notices of the Royal Astronomical Society, 492, 2828–2834

Matteucci F., 2014, in Bland-Hawthorn J., Freeman K., Matteucci F., eds, Saas-Fee Advanced Course Vol. 37, Saas-Fee Advanced Course. p. 145 (`arXiv:0804.1492`), doi:10.1007/978-3-642-41720-7_2

Ritter C., Côté B., 2016a, NuPyCEE: NuGrid Python Chemical Evolution Environment, Astrophysics Source Code Library, record ascl:1610.015

Ritter C., Côté B., 2016b, NuPyCEE: NuGrid Python Chemical Evolution Environment, Astrophysics Source Code Library, record ascl:1610.015

Ritter C., Côté B., Herwig F., Navarro J. F., Fryer C. L., 2018a, ApJS, 237, 42

Ritter C., Herwig F., Jones S., Pignatari M., Fryer C., Hirschi R., 2018b, Monthly Notices of the Royal Astronomical Society, 480, 538

van Raai, M. A. Lugaro, M. Karakas, A. I. García-Hernández, D. A. Yong, D. 2012, A&A, 540, A44